

See discussions, stats, and author profiles for this publication at: <https://www.researchgate.net/publication/227769356>

# Cure kinetics of epoxy resins and aromatic diamines

Article in *Journal of Applied Polymer Science* · August 1986

DOI: 10.1002/app.1986.070320231

CITATIONS

124

READS

2,057

4 authors, including:



Antonio Moroni

Cordis Health

12 PUBLICATIONS 258 CITATIONS

[SEE PROFILE](#)



Eli M Pearce

Polytechnic Institute of New York University

221 PUBLICATIONS 5,488 CITATIONS

[SEE PROFILE](#)

Some of the authors of this publication are also working on these related projects:



Polymer Characterization [View project](#)



Epoxy Curing [View project](#)

# Cure Kinetics of Epoxy Resins and Aromatic Diamines

ANTONIO MORONI, JOVAN MIJOVIC,\* ELI M. PEARCE, and  
CHEU CHING FOUN, *Departments of Chemistry, and Chemical  
Engineering, and the Polymer Research Institute, Polytechnic Institute of  
New York, 333 Jay Street, Brooklyn, New York 11201*

## Synopsis

An analysis of the cure kinetics of several different formulations composed of bifunctional epoxy resins and aromatic diamines was performed. A series of isothermal differential scanning calorimetry (DSC) runs (at higher temperature) and Fourier transform infrared spectroscopy (FT-IR) runs (at lower temperature) provided information about the kinetics of cure in the temperature range 18–160°C. All kinetic parameters of the curing reaction, including the reaction rate order, activation energy, and frequency factor were calculated and reported. Dynamic and isothermal DSC yielded different results. An explanation was offered in terms of different curing mechanisms which prevail under different curing conditions. A mechanism scheme was proposed to account for various possible reactions during cure.

## INTRODUCTION

Epoxy resins are widely used as adhesives and as the matrix material for high performance composites in the aerospace industry. Linear epoxy resins are converted into a three-dimensional cross-linked thermoset network during cure. Various chemical reactions that take place during cure determine the resin morphology which, in turn, determines the properties of the cured formulation. An understanding of the mechanism and rate (kinetics) of cure is needed to establish processing–morphology–property relationships in thermosets and their composites.

An excellent review of the kinetics of cure of thermosetting resins has been written by Prime.<sup>1</sup> Various other studies, using different experimental techniques, report efforts to evaluate the rate and mechanism of cure. The cure kinetics have been described by both  $n^{\text{th}}$  order<sup>1–6</sup> and autocatalytic mechanisms.<sup>7–11</sup>

Differential scanning calorimetry (DSC) has been the most commonly used experimental technique for curing studies. The objective of this study is to utilize both isothermal and dynamic DSC as well as Fourier transform infrared spectroscopy (FT-IR) to evaluate the mechanism of cure of epoxy formulations. When combined with graphite fibers, the formulations studied herein become promising candidates for filament wound structures in aerospace applications.

\*To whom all correspondence should be addressed.

## BASIC APPROACH

The curing reactions were investigated by differential scanning calorimetry (DSC) under both isothermal and nonisothermal conditions. The heat released during cure, measured as a function of time and temperature, was assumed to be directly proportional to the rate of reaction  $\dot{\alpha}$  (1):

$$\dot{\alpha} = d\alpha/dt = (1/Q_{\text{ult}}) (dQ/dt) \quad (1)$$

The extent of reaction  $\alpha$  was taken as the heat evolved at a certain time ( $Q_t$ ) divided by the total heat of reaction ( $Q_{\text{ult}}$ ):

$$\alpha_t = Q_t/Q_{\text{ult}} \quad (2)$$

Systems cured isothermally below the  $T_{g^x}$  showed an incomplete cure due to vitrification;<sup>12</sup> therefore, the total heat of reaction was taken as:

$$Q_{\text{ult}} = Q_{\text{iso}} + Q_{\text{res}} \quad (3)$$

where  $Q_{\text{iso}}$  is the heat evolved during the isothermal cure and  $Q_{\text{res}}$  is the residual heat released during the dynamic run of the sample after the isothermal cure.

During the isothermal studies, the curing reaction shows a marked autocatalytic behavior, as reported in the literature.<sup>8</sup> The curing reaction may be successfully described by the following kinetic equation:<sup>7,8,11</sup>

$$\dot{\alpha} = d\alpha/dt = (k_1 + k_2\alpha^m)(1 - \alpha)^n \quad (4)$$

where  $k_1$  and  $k_2$  are kinetic rate constants and  $m + n$  the overall reaction order. The overall reaction order is assumed to be two thus expressing a pseudosecond order mechanism which takes place in systems where the concentration of OH groups is fairly high.<sup>12</sup> This equation can successfully describe the autocatalytic behavior shown during cure when the amounts of amine hydrogens and epoxide groups are in the vicinity of the stoichiometric ratio.

Curing kinetics were also investigated by nonisothermal (dynamic) DSC at different heating rates. The activation energy ( $E_a$ ), frequency factor ( $A$ ), and order of reaction ( $n$ ) were calculated using the Borchardt-Daniels method<sup>14</sup> applied to the following kinetic equation:

$$\dot{\alpha} = d\alpha/dt = A \exp(-E_a/RT) (1 - \alpha)^n \quad (5)$$

where  $n$  is the reaction rate order.

The extent of conversion of the epoxy resin was also followed as a function of the time and temperature of cure by FT-IR monitoring the disappearance of the  $915 \text{ cm}^{-1}$  band characteristic of the epoxy ring, normalized to an internal reference band at  $1184 \text{ cm}^{-1}$ . Details of this procedure are given

elsewhere.<sup>15</sup> Using this technique plots of the conversion as a function of time were drawn for several isothermal runs in the range 18–120°C.

## EXPERIMENTAL

The formulations used in this study were based on an 80/20 mixture of a DGEBA resin (diglycidyl ether of bisphenol A, Shell's Epon 826) containing a small amount of higher oligomeric fractions (8.7%), and a DGBE-reactivity epoxy diluent (diglycidyl ether of 1,4-butanediol, Celanese's Epirez 5022) containing pure GBE (51.2%) and higher oligomeric fractions ( $n = 1$ , 34.3%;  $n = 2$ , 9.2%;  $n \geq 3$ , 4.3%). The DGEBA/DGBE mixture was cured with a mixture of aromatic di- and polyamines (meta-phenylenediamine, 42%; methylenedianiline, 42%; 2,4-bis(aminobenzyl)aniline, and oligomers, 16%).

The epoxy-amine mixtures were prepared at room temperature in the amine/epoxy ratios of A/E = 1.0 (Formulation A) and 1.1 (Formulation B) by adding the curing agent while continuously stirring until a homogeneous solution was obtained. The solution was then degassed under vacuum and samples (7–9 mg) were prepared, sealed in hermetic aluminum pans, and tested immediately. Samples aged even a few hours at room temperature gave unreliable results due to the onset of a slow curing reaction.

A Du Pont 1090 Thermal Analyzer connected to a 910 DSC module was used to measure the heat flow as a function of time after calibration with high purity Indium (Du Pont thermometric standard). Dynamic experiments were run in the range –60 to 300°C. Isothermal experiments were conducted in the temperature range 70–150°C. Isothermally cured samples were then quenched and scanned from –60 to +300°C at a heating rate of 10°C per minute to measure  $Q_{\text{res}}$ .

A steady isothermal baseline was established at the preset curing temperature using two empty sample pans. The sample pan was then introduced in the DSC cell and the data acquisition initiated. Thermal equilibrium between sample and reference pans was achieved in less than one minute from the start of reaction. The reaction was considered to be complete when the rate curve levelled off to the baseline. Data collected by DSC were processed by a Digital PDP-1170 computer to obtain the rate  $\dot{\alpha}$  and extent of cure  $\alpha$  as a function of time.

The kinetic parameters of Eq. (4) were calculated using a nonlinear regression of the reduced reaction rate  $\dot{\alpha}/(1 - \alpha)^n$  over  $\alpha^m$  in a range of conversion where there is no influence of the diffusion control on the rate of reaction. The inaccuracy of the measurement of  $(\dot{\alpha})_{t=0}$  due to the lack of thermal equilibrium during the first stage of analysis is taken into account and corrected. Finally, using data collected during cure at different temperatures, the activation energies, frequency factors, and temperature dependence of the order of reaction are determined.

The flowchart of the computer program used for these purposes is shown in Figure 1.

The curing kinetics at low temperatures where DSC measurements are affected by an experimental error were also investigated by FT-IR by fol-

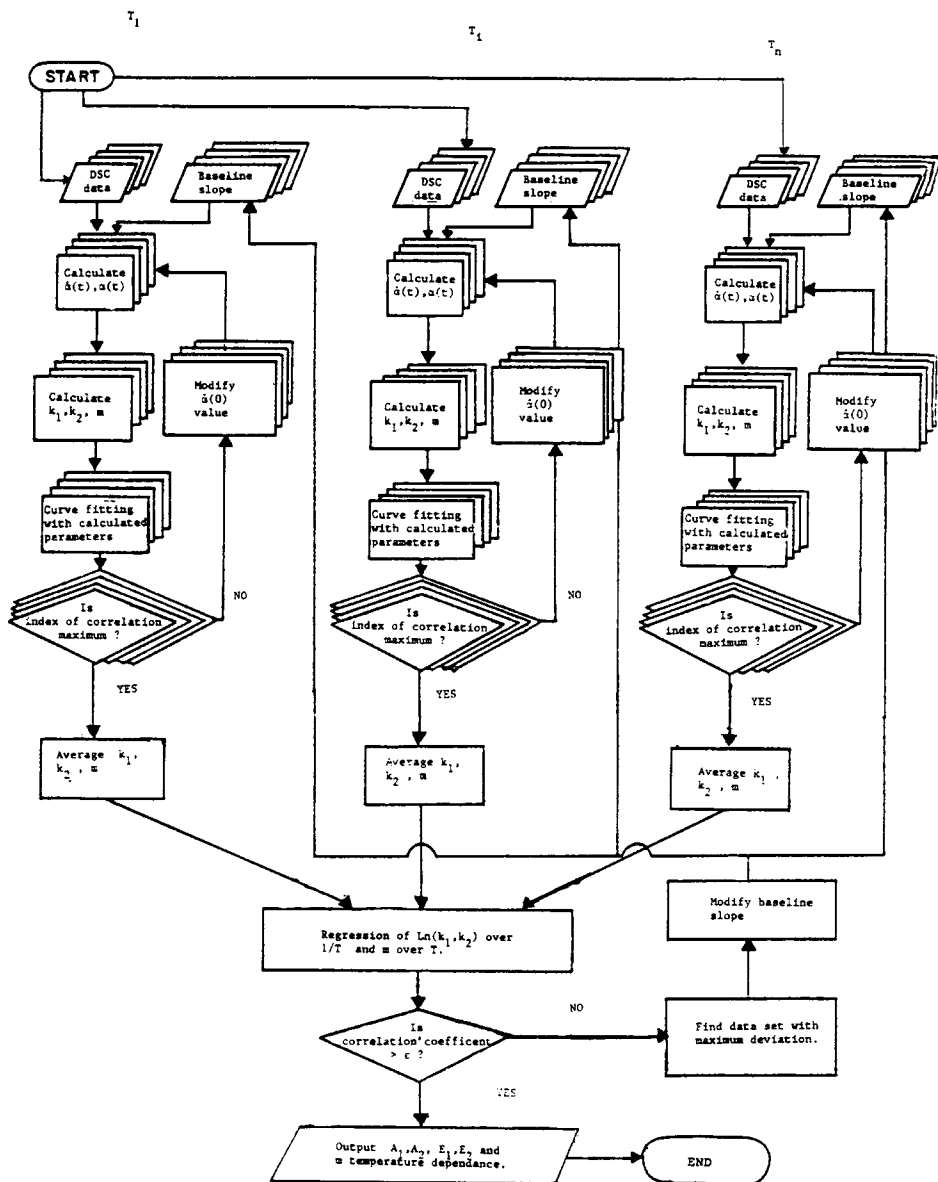


Fig. 1. Flowchart of the computer program used to calculate kinetic parameters of the curing reaction.

lowing the change in the absorbance ratio  $A_{915}/A_{1184}$ .<sup>15</sup> In the FT-IR case the study of the curing reaction was based on the determination of time to reach a conversion of 50%.

## RESULTS AND DISCUSSION

A series of isothermal reaction rate curves for formulation A are shown in Figure 2. With a decrease in cure temperature a decrease in the peak

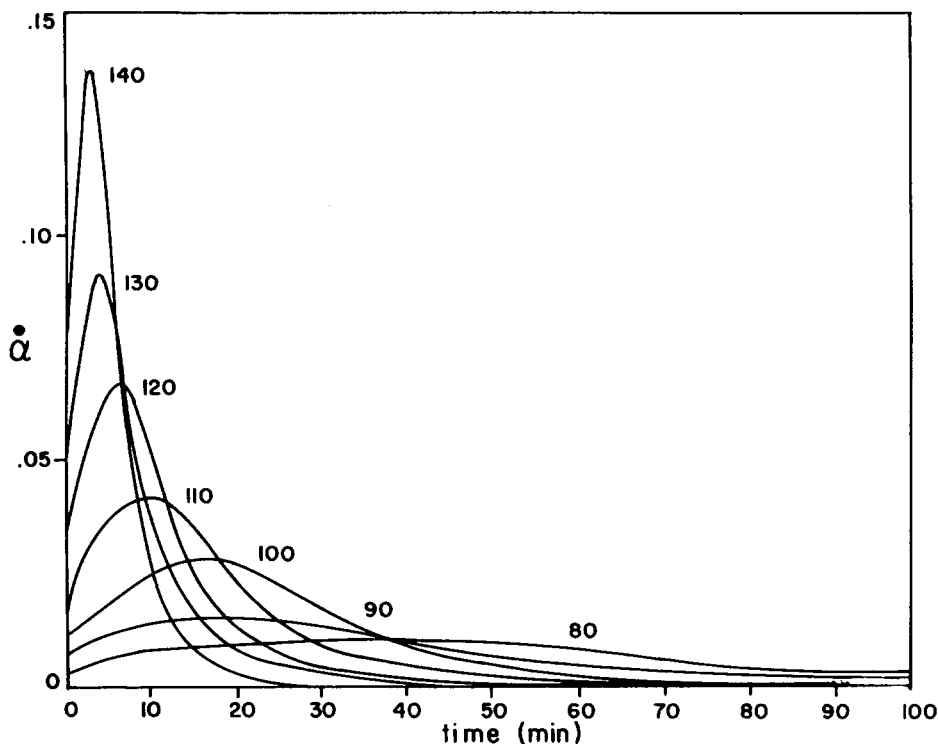


Fig. 2. Rate of reaction as a function of time at several isothermal temperatures. Formulation A.

value of the reaction rate ( $\dot{\alpha}_p$ ) and its shift to longer times were observed. The extent of reaction ( $\alpha$ ) was next plotted as a function of curing time and the resulting curves are shown in Figure 3. The sigmoidal shape of these curves suggests the autocatalytic curing kinetic mechanism in these systems. Both formulations studied, A and B, show similar behavior. The observed differences in the temperature dependence of values of rate constants ( $k_1, k_2$ ) and of the time to 50% conversion are summarized in Tables I and II.

Plots of reduced reaction rate vs. extent of reaction (Fig. 4) were used to calculate  $k_1$  and  $k_2$ , from the intercept and the slope of the linear part of the curve, respectively, using Eq. (4). Figure 4 also shows that curing reactions are quenched by vitrification when the system is cured below the glass transition temperature of the fully cured system ( $T_{gx}$ ).  $T_{gx}$  is defined as the temperature of transition from the liquid or rubbery state to the glassy state for a fully cured system and it was found to be in the range 105–115°C in our study. Both kinetic rate constants  $k_1$  and  $k_2$  obey the classical Arrhenius form as shown in Figure 5. As previously stated, the overall order of reaction ( $m + n$ ) was assumed to be two. The value of ( $m$ ) appears to pass through a maximum between 90° and 110°C as seen in Figure 6, contrasting with some results reported earlier where a linear or exponential dependence of ( $m$ ) was observed.<sup>9</sup>

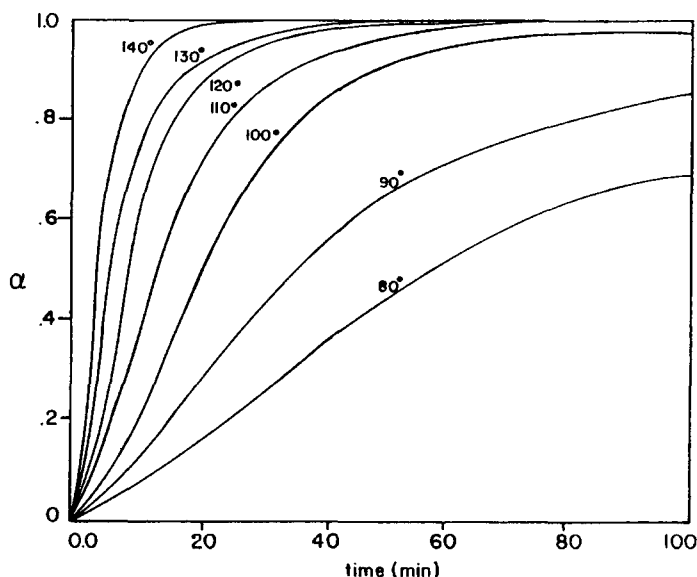


Fig. 3. Extent of reaction as a function of time at several isothermal temperatures. Formulation A.

The results of our kinetic analysis indicate the presence of more than one type of kinetic mechanism. The primary reaction occurs with an activation energy of about 13.5 kcal/mole and a kinetic exponent ( $n$ ) in the range 1.1–1.3. This reaction may be described as a catalytic ring opening by the primary amino groups, involving a ternary transition state amine-epoxide-hydrogen donor present in the reaction medium.

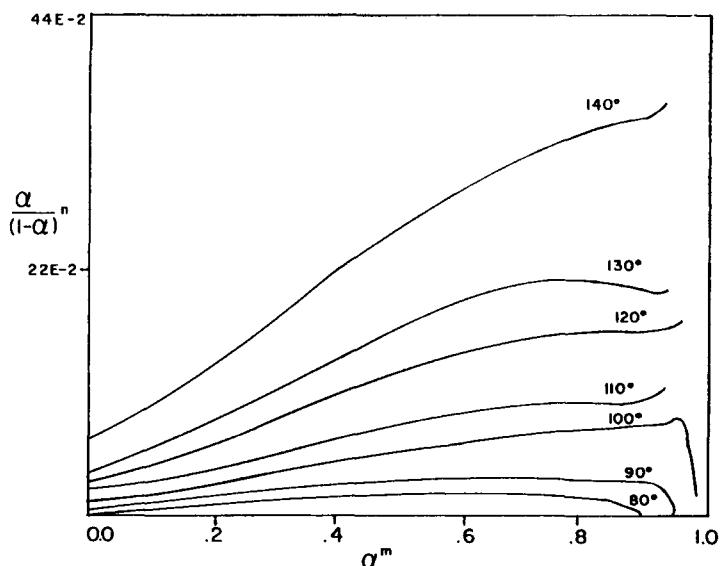


Fig. 4. Reduced reaction rate  $\alpha/(1 - \alpha)^n$  as a function of  $\alpha^m$  for several isothermal temperatures.

TABLE I  
Temperature Dependence of the Kinetic Parameters for Isothermal Cure Analysis of  
Formulation A (DGEBA/DGBE (80/20) Mixture Cured with Tonox 60/40.  $A/E = 1.0$ )

| Kinetic parameter | Temperature dependence                   | Correlation coefficient |
|-------------------|--|-------------------------|
| $k_1$             | $1.03 \cdot 10^6 \cdot \exp(13.5/RT)$    | .9965                   |
| $k_2$             | $7.26 \cdot 10^5 \cdot \exp(11.9/RT)$    | .9933                   |
| $t_{50}$          | $5.21 \cdot 10^{-7} \cdot \exp(13.1/RT)$ | .9996                   |

TABLE II  
Temperature Dependence of the Kinetic Parameters for Isothermal Cure Analysis of  
Formulation B (DGEBA/DGBE (80/20) Mixture Cured with Tonox 60/40.  $A/E = 1.1$ )

| Kinetic parameter | Temperature dependence                   | Correlation coefficient |
|-------------------|--|-------------------------|
| $k_1$             | $1.16 \cdot 10^6 \cdot \exp(13.6/RT)$    | .9990                   |
| $k_2$             | $9.63 \cdot 10^5 \cdot \exp(12.0/RT)$    | .9971                   |
| $t_{50}$          | $8.26 \cdot 10^{-7} \cdot \exp(12.7/RT)$ | .9998                   |

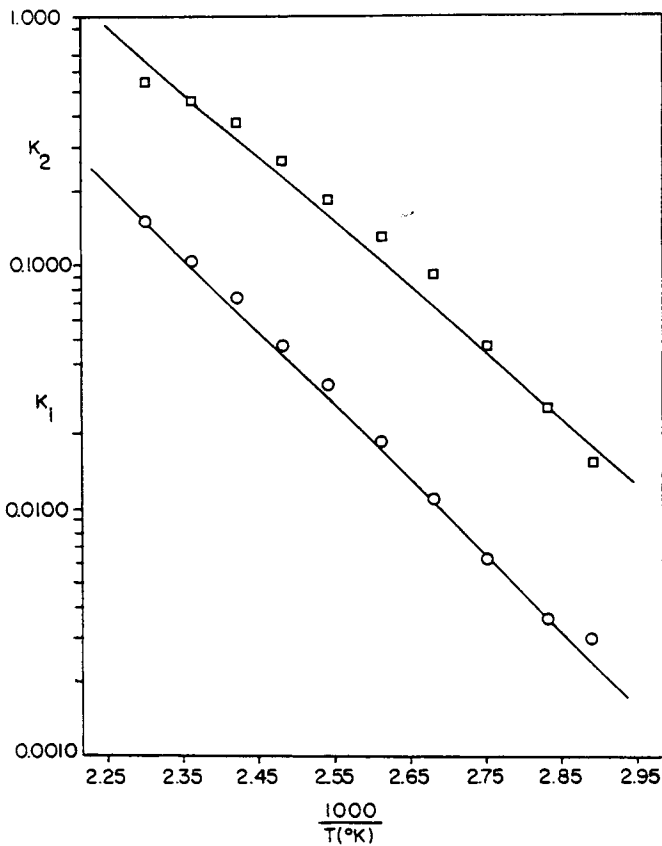


Fig. 5. Temperature dependence of the kinetic constants  $k_1$  and  $k_2$ ; Formulation A:  $k_1$  ○,  $k_2$  □.



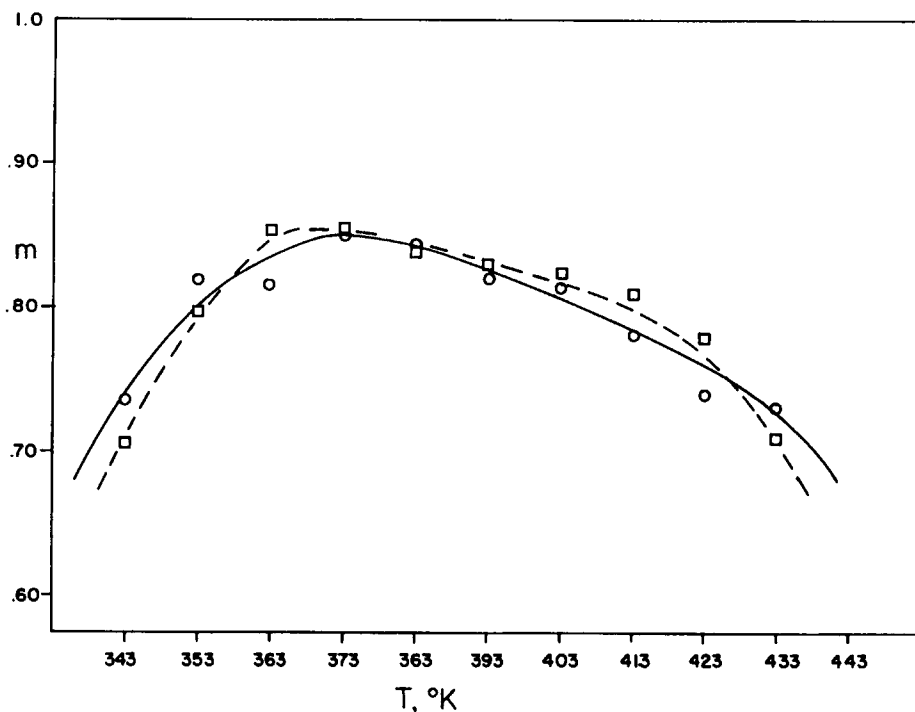


Fig. 6. Temperature dependence of the kinetic exponent  $m$ ; Formulation A  $\Delta$ ; Formulation B  $\square$ .

As reported in the literature,<sup>13</sup> the epoxide ring opening follows a second-order mechanism with aliphatic amines. A reaction order between one and two is observed in the ring opening by acidic media, where the attachment of the weaker nucleophile is assisted by protonation of the oxirane.<sup>16</sup> In case of aromatic amines, usually weaker than aliphatic, the ring-opening reaction appears to be catalyzed by hydrogen donor groups present in the system, thus being similar to the reaction discussed above and explaining the value obtained for the kinetic exponent ( $n$ ). The second type of reaction has an activation energy of about 12 kcal/mole. This subsequent reaction most likely comprises a catalytic ring opening due to the secondary amine formed with the transition state similar to the one described above, and a true autocatalytic ring opening involving a secondary amine, an epoxide and a hydroxyl group formed *in situ* by the opening of the first epoxy ring.

The transition state of this last reaction may be arranged in a seven-member ring, thus explaining the lower activation energy.

These two different reactions take place to a different extent depending on the curing temperature and are responsible for the convex shape of the curve describing the temperature dependence of the kinetic constant  $k_2$ , shown in Figure 5, the reaction being faster when a higher fraction of the subsequent reaction follows the autocatalytic path. The kinetic exponent ( $m$ ) represents the quantitative measure of how much of the subsequent curing reactions follow the autocatalytic path. The observed complicated dependence of  $k_2$  and  $m$  on the curing temperature, with a maximum in a relatively

narrow temperature range, points out the difficulty in forming a large amount of the low energy cyclic transition state. This is true at both low and high temperatures.

A departure from the stoichiometric ratio (Formulation B) increases the rate of the curing reaction; however the difference in the values of  $k_1$  and  $k_2$  was quite small and a considerable overlap occurred. Hence, data from Formulation B were not plotted in Figure 5. The  $E_1$  value does not change to a large extent while  $A_1$  increases by increasing the concentration of amino groups.  $E_2$  values are also similar for the two formulations and  $A_2$  increases by increasing the  $A/E$  ratio.

As seen in Figure 4, the onset of the diffusion control of curing reactions in the vicinity of the gel point slows down the rate of reaction. This is a consequence of the formation of a cross-linked network characterized by the presence of rigid aromatic rings which exist both in the epoxy resin and in the curing agent. It is worth mentioning here that our results contrast with studies done on similar resin systems<sup>7,17</sup> but cured with more flexible aliphatic diamines, where the rate of reaction was not found to decrease after the gel point.

In systems cured above  $T_{g\infty}$  the  $Q_{iso}$  evolved during cure did not change as a function of temperature outside the error range of the technique. Systems cured below  $T_{g\infty}$  showed lower  $T_g$  and an amount of  $Q_{res}$  which is related to the inverse function of the curing temperature.

$Q_{res}$  is assumed to be the heat of reaction not released by the system when the vitrification prevents the curing reaction from going to completion and it is measured as reported<sup>10</sup> and described in the experimental part.

Figure 7 shows the amount of  $Q_{res}$  released by the subsequent dynamic scans of isothermally cured systems and their  $T_g$ 's. For the formulation A

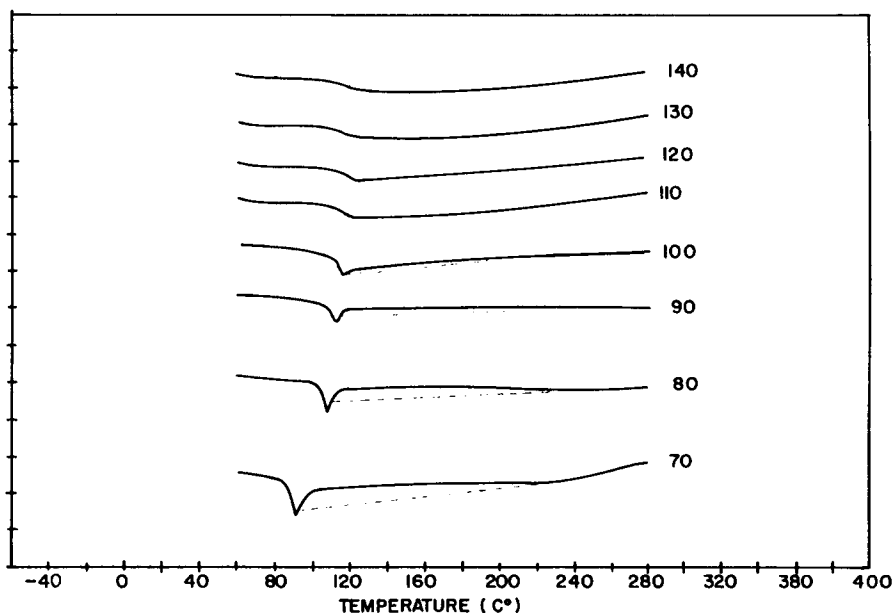


Fig. 7.  $T_g$  and  $Q_{res}$  released by Formulation A after isothermal cure.

( $A/E = 1.0$ )  $T_{g^\infty}$  (onset, 105°C) is slightly lower than that of Formulation B ( $A/E = 1.1$  onset, 115°C). It is also worth noting that  $T_g$  as a function of the conversion approaches  $T_{g^\infty}$  more rapidly for formulation B. Also,  $Q_{res}$  of samples of B cured below  $T_{g^\infty}$  has a higher value and increases more quickly as an inverse function of the isothermal curing temperature when compared to the samples of Formulation A. The higher reaction heat evolved during cure of Formulation B above the  $T_{g^\infty}$ , and a different dependence of  $T_g$  on conversion, indicate the formation of a tighter cross-linked network in this case.

In the next series of experiments, dynamic differential scanning calorimetry was employed to study the curing kinetics of Formulation A. Interestingly, it was found that when the system is tested in the dynamic mode a unique activation energy is sufficient to describe the cure process [Eq. (5)].

Our measurements yield an activation energy of  $22.3 \pm 0.2$  kcal/mole and a reaction order of 1.45. The summary of kinetic parameters obtained from a series of dynamic runs is given in Table III. The values of  $E_a$  and  $n$  are slightly lower than those reported for similar systems.<sup>7,10</sup>

The results obtained from nonisothermal runs may be explained by the occurrence of a noncatalytic ring-opening mechanism, probably because of the difficulty of formation of the ternary complex amine-epoxide-hydrogen donor<sup>7,10</sup> due to the constant flow of thermal energy furnished to the system. An FT-IR spectrum of the band characteristic of the epoxy ring at  $915\text{ cm}^{-1}$  (Fig. 8) shows the peak shifted to lower wavelengths when the system is cured isothermally versus dynamically. This result suggests that some hydrogen bonding takes place during the isothermal cure but not during the dynamic cure.

Next, data obtained from both the integral DSC plots shown in Figure 2 and from the FT-IR spectra were reduced to calculate the activation energy of the curing reaction for Formulation B in the temperature range 18–160°C. Assuming an Arrhenius relationship, a semilogarithmic plot of time to reach a certain conversion versus  $1/T$  shall have a slope equal to  $E_a/R$  (Fig. 9). Activation energies of 13.1 and 12.7 kcal/mole were measured for Formulation A and B, respectively and both techniques yield agreeable results.

TABLE III

Results from Dynamic Cure Analysis of Formulation A (DGEBA/DGBE (80/20) Mixture Cured with Tonox 60/40.  $A/E = 1.0$ ). Data reduction performed in the conversion range 6–65%.

| Heating rate | $E_a$<br>kcal/mole | $A$<br>$\text{min}^{-1}$ | $n$  |
|--------------|--------------------|--------------------------|------|
| 2            | 22.3               | $3.69 \cdot 10^{11}$     | 1.55 |
| 4            | 22.2               | $1.66 \cdot 10^{11}$     | 1.45 |
| 8            | 22.4               | $1.40 \cdot 10^{11}$     | 1.40 |
| 10           | 22.1               | $7.67 \cdot 10^{10}$     | 1.45 |
| 12           | 22.6               | $1.02 \cdot 10^{11}$     | 1.40 |
| 16           | 22.3               | $5.48 \cdot 10^{10}$     | 1.40 |
| 20           | 22.3               | $4.98 \cdot 10^{10}$     | 1.40 |

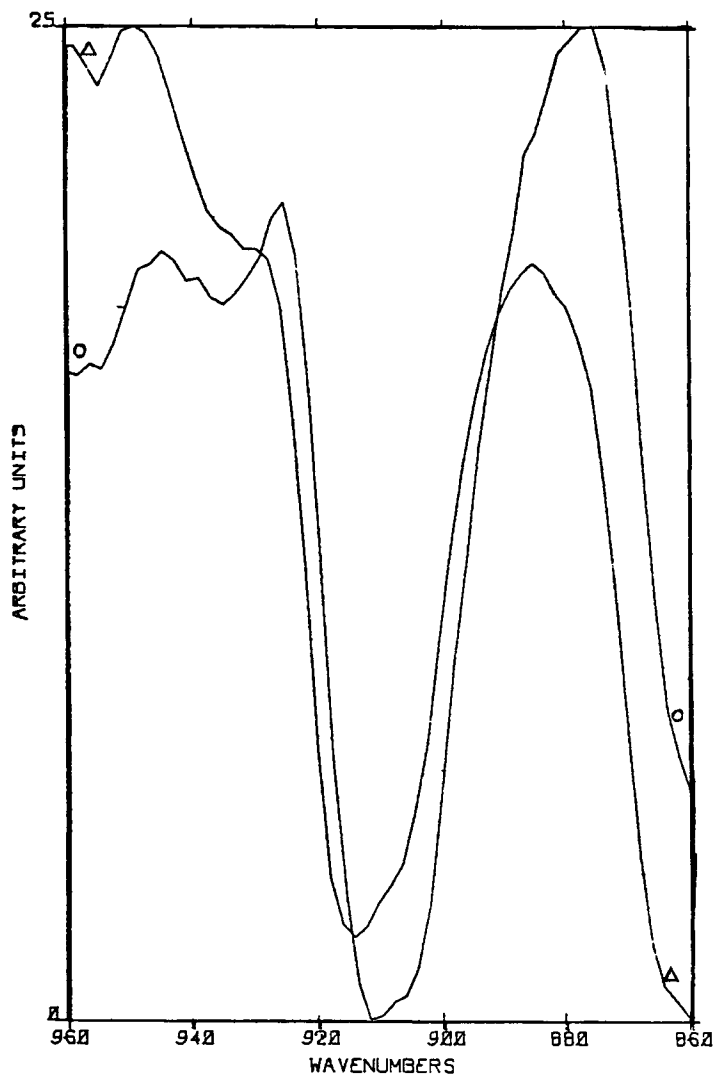


Fig. 8. FT-IR spectra of the  $915\text{ cm}^{-1}$  oxirane band during isothermal ○ and dynamic Δ cure.

The techniques described, where only the extent of reaction can be measured with high accuracy, calculate a global activation energy and do not distinguish between different types of reaction. However, using low curing temperatures where the autocatalytic nature of the reaction decreases, a unique kinetic parameter can describe cure with sufficient accuracy.

The analysis of the results obtained in this study suggests that the curing reaction may follow different paths depending on the curing conditions. A proposed mechanism for various possible curing reactions is shown in Figure 10.

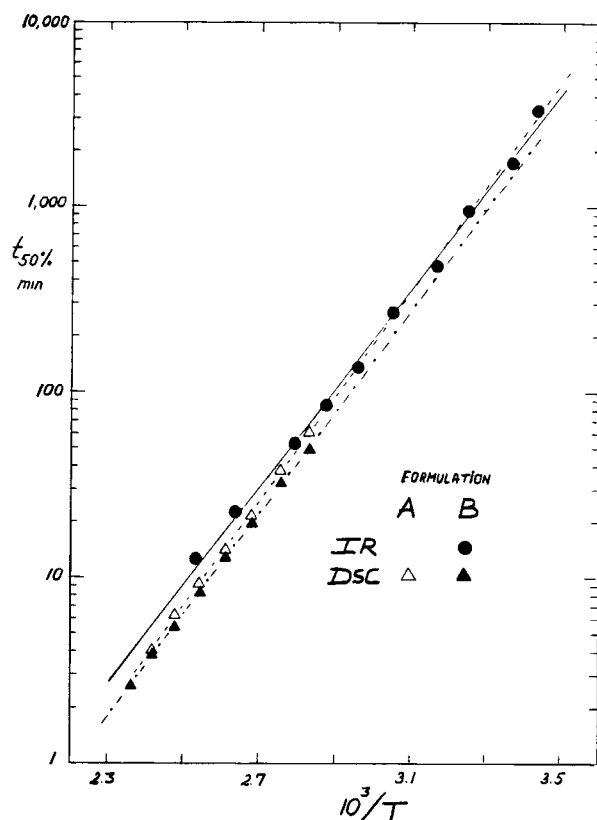


Fig. 9. Temperature dependence of  $T_{50}$ ; Formulation A,  $\Delta$  (DSC), Formulation B,  $\blacktriangle$  (DSC),  $\bullet$  (FT-IR).

## CONCLUSIONS

The results of this study suggest the presence of several different mechanisms during cure of an epoxy formulation. Thermal analysis data, integrated by an appropriate mathematical treatment, allowed us to distinguish between different kinetic mechanisms. Kinetic parameters, including the order of reaction, activation energy, and frequency factor were calculated. The occurrence of different curing mechanisms under different conditions was used to explain the discrepancy between results obtained in isothermal vs. dynamic DSC. Phase transitions also have a strong influence on the curing mechanism.

FT-IR studies provided useful information about cure at lower temperature and yielded results in good agreement with DSC. Furthermore, as the autocatalytic mode of the reaction decreases at lower curing temperatures, the distinction between primary and subsequent reactions becomes less pronounced. Then the curing kinetics can be successfully described by only one reaction rate constant obtained from measurements of conversion as a function of time.

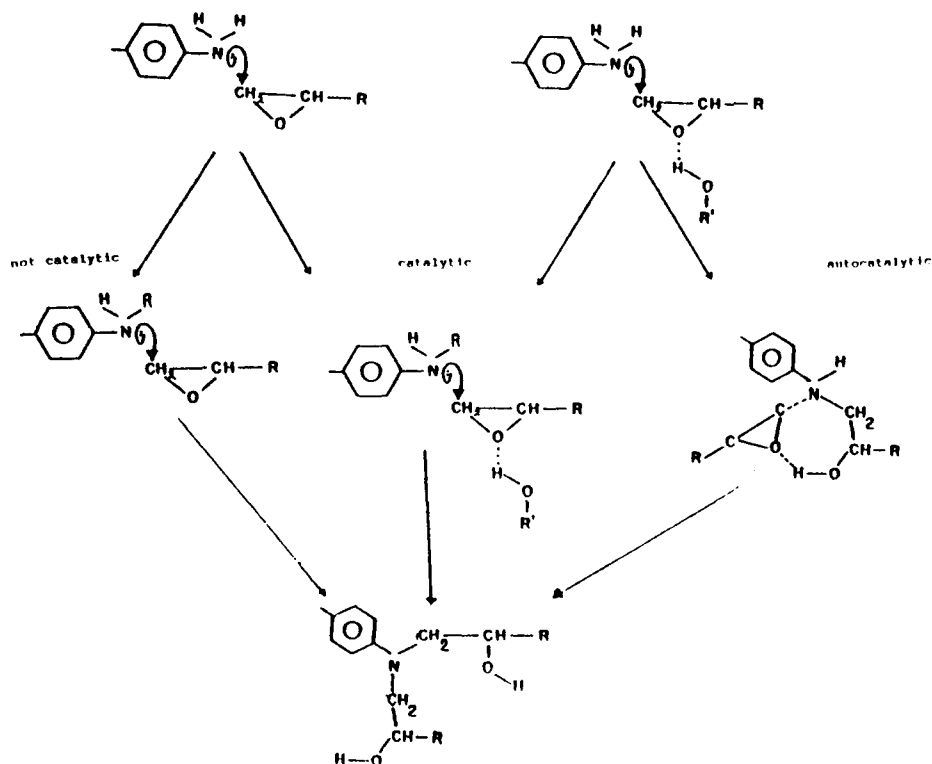


Fig. 10. Proposed cure mechanisms of epoxy resins and aromatic diamines.

The authors acknowledge support of this work by NASA-Ames Research Center, under Grant NAG 2-229. The authors thank Dr. M. A. Golub at that Center for helpful discussions.

## References

1. R. B. Prime, *Thermal Characteristics of Polymeric Materials*, E. Turi, Ed., Academic Press, New York, 1982, Ch. 5.
2. M. A. Acitelli, R. B. Prime, and E. Scalt, *Polymer*, **12**, 335 (1971).
3. T. Donellan and D. Roylance, *Polym. Eng. Sci.*, **22**(13), 821 (1982).
4. N. S. Schneider, J. F. Sprouse, G. L. Hagnauer, and J. K. Gillham, *Polym. Eng. Sci.*, **19**, 304 (1979).
5. R. B. Prime, *Anal. Calorim.*, **2**, 201 (1970).
6. R. B. Prime, *Polym. Eng. Sci.*, **13**, 453, (1973).
7. K. Horie, H. Hiura, M. Sawada, I. Mita, and H. Kambe, *J. Polym. Sci.*, **A-1**, **8**, 1357 (1970).
8. S. Sourour and M. R. Kamal, *Thermochimica Acta*, **14**, 41 (1976).
9. M. E. Ryan and A. Dutta, *Polymer*, **20**, 203 (1979).
10. C. C. Riccardi, H. E. Adabbo, and R. R. J. Williams, *J. Appl. Polym. Sci.*, **29**, 2481 (1984).
11. J. Mijovic, J. Kim, and J. Slaby, *J. Appl. Polym. Sci.*, **29**, 1449 (1984).
12. J. B. Enns and J. K. Gillham, *J. Appl. Polym. Sci.*, **28**, 2567-91 (1983).
13. I. T. Smith, *Polymer*, **2**, 95 (1961).
14. J. Borchardt and F. Daniels, *J. Am. Chem. Soc.*, **79**, 41 (1957).
15. M. A. Golub, N. R. Lerner and M. S. Hsu, *J. Appl. Polym. Sci.*, in press.
16. E. S. Gould, *Mechanisms and Structure in Organic Chemistry*, Holt, Rinehart and Winston, New York, 1959, p. 291.
17. S. Lunak and K. Dusek, *J. Polym. Sci., Polym. Symp.*, **53**, 29 (1976).